Pek-Lan Khong, FRCR
Lucullus H. T. Leung, PhD
Godfrey C. F. Chan, FRCP
Dora L. W. Kwong, FRCR
Wilfred H. S. Wong, MMedSc
Guang Cao, PhD
Gaik-Cheng Ooi, FRCR

**Published online**
10.1148/radiol.2362041066
**Radiology 2005;** 236:647–652

**Abbreviations:**
CSF = cerebrospinal fluid
CSI = craniospinal irradiation
FA = fractional anisotropy
ΔFA = percentage change in WM FA
SPM = statistical parametric mapping
WM = white matter

[1] From the Departments of Diagnostic Radiology (P.L.K., G.C.O.), Clinical Oncology (L.H.T.L., D.L.W.K.), and Paediatric and Adolescent Medicine (G.C.F.C., W.H.S.W.), Queen Mary Hospital, University of Hong Kong, Block K, Room 406, 102 Pokfulam Rd, Hong Kong, China; and GE Medical Systems Asia (G.C.).Received June 16, 2004; revision requested August 25; revision received September 6; accepted October 15. Supported in part by a grant from the Hong Kong Research Grants Council (HKU 7416/03M). **Address correspondence to** P.L.K. (e-mail: *plkhong@hkucc.hku.hk*).

**Author contributions:**
Guarantors of integrity of entire study, all authors; study concepts, P.L.K., L.H.T.L., G.C.F.C., D.L.W.K., G.C.O.; study design, P.L.K., L.H.T.L., G.C.F.C., D.L.W.K., W.H.S.W.; literature research, P.L.K., L.H.T.L.; clinical studies, P.L.K., G.C.F.C., D.L.W.K.; data acquisition, P.L.K., L.H.T.L., G.C.F.C., D.L.W.K.; data analysis/interpretation, P.L.K., L.H.T.L., G.C.F.C., D.L.W.K., W.H.S.W.; statistical analysis, P.L.K., D.L.W.K., W.H.S.W.; manuscript preparation, P.L.K., L.H.T.L., G.C.F.C., D.L.W.K.; manuscript definition of intellectual content, editing, revision/review, and final version approval, all authors



# White Matter Anisotropy in Childhood Medulloblastoma Survivors: Association with Neurotoxicity Risk Factors[1]

**PURPOSE:** To prospectively evaluate the relationships between change in white matter (WM) anisotropy and *(a)* patient age at craniospinal irradiation (CSI), *(b)* CSI dose, and *(c)* time of magnetic resonance (MR) imaging since CSI and to determine the effect of these neurotoxicity risk factors on WM anisotropy in posttreatment medulloblastoma survivors.

**MATERIALS AND METHODS:** Informed consent was obtained from the patients, control subjects, or their parents, and the study was approved by the institutional review board. Twenty consecutive medulloblastoma survivors (14 male, six female; mean age, 11.0 years ± 4.6 [standard deviation]) and 36 control subjects (14 male, 22 female; mean age, 10.7 years ± 3.5) were examined. Control subjects were divided into four groups according to age: 5.0–7.9 years, 8.0–10.9 years, 11.0–13.9 years, and 14.0–18.9 years. The authors calculated the histogram-derived mean WM fractional anisotropy (FA) value for each patient and compared it with the mean WM FA value for the control subjects in the corresponding age group to evaluate the percentage change in WM FA (ΔFA) in each patient. Spearman rank correlation analysis was used to analyze the relationships between ΔFA and *(a)* age at CSI, *(b)* CSI dose, and *(c)* time of MR imaging since CSI. Then, multiple linear regression analysis was performed to study the simultaneous influence of these factors on ΔFA.

**RESULTS:** There were significant correlations between ΔFA and both age at CSI ($r = 0.631$, $P = .003$) and CSI dose ($r = -0.586$, $P = .007$) but not between ΔFA and time of MR imaging since CSI. Multiple linear regression analysis revealed age at CSI to be the only independent variable that significantly affected ΔFA (adjusted $r^2 = 0.391$, $P = .012$).

**CONCLUSION:** Loss of WM anisotropy is significantly affected by age at CSI, and there is a trend toward increasing anisotropy loss with larger CSI dose. Both age at CSI and CSI dose are known risk factors of neurotoxicity.


The long-term survival of patients with medulloblastoma has improved considerably since the advent of multimodality treatments. With the increased numbers of survivors, greater attention to the quality of survival for these patients is needed. Treatment-induced neurotoxicity—mainly that resulting from the deleterious effects of whole-brain irradiation on the white matter (WM)—is prevalent and manifests as diverse forms of cognitive dysfunction (1–4). However, because cognitive assessment of neurobehavioral morbidity is considered to be a late-outcome measurement, the identification of earlier and more sensitive markers of neurologic development and neurotoxicity is necessary. With the identification of these markers, there is the potential to limit or more effectively time (at developmentally advantageous points) neurotoxic treatments.

We previously have found, by using diffusion-tensor magnetic resonance (MR) imaging, that fractional anisotropy (FA) is reduced in the WM of childhood medulloblastoma

survivors after craniospinal irradiation (CSI) and chemotherapy (5,6). This finding suggests that anisotropy loss may be used as an indicator of treatment-induced neurotoxicity. Although the mean diffusivity value was increased in the medulloblastoma survivors compared with that in the healthy control subjects, the difference was not statistically significant; thus, diffusivity was considered to be less sensitive than FA for the detection of treatment-induced WM damage (5). Histopathologic and cognitive study results have shown that neurotoxic effects are more severe in the maturing brain and with higher radiation doses (7–16). Thus, the purposes of our study were to prospectively evaluate the relationships between change in WM anisotropy and the factors patient age at CSI, CSI dose, and time of MR imaging examination since CSI and to determine the effect of these neurotoxicity risk factors on WM anisotropy in posttreatment medulloblastoma survivors.

## MATERIALS AND METHODS

### Patient Data

Patients with childhood medulloblastoma who had been healthy and developing normally before the tumor diagnosis were referred from the pediatric oncology unit of our hospital for enrollment in this study. Informed consent was obtained from all patients or their parents, and the study was approved by our institutional review board. Twenty-two consecutive medulloblastoma survivors were recruited for this cross-sectional study. Two patients were subsequently excluded from the study cohort: one because of failed statistical parametric mapping (SPM) segmentation due to markedly dilated ventricles and the other because of poor compliance with the treatment protocol and frequent defaults on follow-up visits that led to treatment delays. Thus, the final study cohort included 20 patients. Fifteen of these 20 patients were a part of our previous study cohort (6). All children underwent tumor resection, CSI, and chemotherapy.

The entire brain was irradiated with doses of up to 23.4–40.0 Gy with lateral opposing fields; radiation was delivered in daily fractions of 1.8–2.0 Gy. Afterward, an additional radiation boost was delivered to the posterior cranial fossa with reduced lateral opposing fields. The total radiation dose to the posterior cranial fossa ranged from 50.0 to 55.8 Gy. The total CSI dose delivered was 23.4 Gy in three, 30.6 Gy in six, 36.0 Gy in nine, and 40.0 Gy in two patients. The patients' ages at CSI ranged from 2.9 to 17.4 years (mean age, 8.6 years ± 4.2 [standard deviation]), and the time between MR imaging examination and CSI ranged from 0.2 to 5.8 years (mean interval, 2.4 years ± 1.9). The patients who received a diagnosis of medulloblastoma before the year 2000 underwent a chemotherapy regimen that consisted of vincristine, cyclophosphamide, cisplatin, and etoposide; these agents used together were referred to as the Pediatric Oncology Group protocol. Those patients who received a diagnosis of medulloblastoma after the year 2000 underwent a chemotherapy regimen that consisted of lomustine, cisplatin, and vincristine; these agents used together were referred to as the CCV protocol.

### Control Subject Data

Thirty-six healthy age-matched subjects served as control subjects after informed consent was obtained from them or their parents. Institutional review board approval to examine these subjects was obtained, as well. These subjects were scheduled to undergo MR imaging of the brain for clinical indications such as headache and congenital sensorineural hearing loss and subsequently confirmed to have normal MR imaging findings and no neurologic deficits at clinical examination. These control subjects were imaged with the same diffusion-tensor MR imaging protocol that was used to image the patients (described below) and were divided into four groups according to their age: Group A comprised seven subjects aged 5.0–7.9 years; group B, 15 subjects aged 8.0–10.9 years; group C, eight subjects aged 11.0–13.9 years; and group D, six subjects aged 14.0–18.9 years.

### Data Acquisition

MR imaging was performed by using a 1.5-T system (Signa; GE Medical Systems, Milwaukee, Wis) with a standard head coil. The following diffusion-tensor MR imaging protocol was used in all control subjects and patients: Diffusion-tensor data were acquired by using single-shot spin-echo echo-planar MR imaging with 10 000/100 (repetition time msec/echo time msec), an acquisition matrix of 128 × 128, and a field of view of 28 cm. By using a section thickness of 5 mm with a 1.5-mm intersection gap, images of the entire brain (comprising about 18 or 19 images) were acquired. Diffusion-sensitizing gradient encoding (17,18) was applied in 25 directions by using a $b$ of 1200 sec/mm$^2$, and one image was acquired without using a diffusion gradient—that is, by using a $b$ of 0. Twenty-six images were obtained at each section of the brain to yield a total of 468 or 494 images. The diffusion-tensor MR imaging time was approximately 5 minutes. To minimize eddy current–related image distortion, we implemented zero and first-order eddy current compensations into the MR imaging system and monitored and calibrated the eddy current level.

### MR Image Data Processing and SPM Analysis

To obtain FA maps, we processed the diffusion-tensor MR image data by using the Functool software program (GE Medical Systems). The diffusion-weighted images were visually inspected (by P.L.K. and L.H.T.L. in consensus) for apparent artifacts due to subject motion, eddy current–related distortion, and instrument malfunction. All image manipulations were performed by using SPM99 (Wellcome Department of Cognitive Neurology, Institute of Neurology, London, England) and Matlab, version 6.5 (The MathWorks, Natick, Mass), software. SPM99 software was used to create the non–diffusion-weighted MR image template and to segment the brain images.

### MR Image Template

A T1-weighted pediatric MR imaging template (CCHMC2_fp; Cincinnati Children's Hospital Medical Center, Cincinnati, Ohio) and its associated a priori probability maps were used in this study because the adult brain imaging template that was available with the SPM99 software was less appropriate for our study cohort of young subjects owing to differences in the size and shape of the brain between children and adults (19). Because T1-weighted MR images were not obtained in all of the control subjects, we created an SPM-template-space non–diffusion-weighted ($b$ = 0) image template. This template had the advantage of preserving the specific regional characteristics that were inherent in the data.

To create the non–diffusion-weighted ($b$ = 0) MR image template, we randomly selected four control subjects and four age-matched patients—one from each age group—with available T1-weighted images to avoid introducing unnecessary bias to-

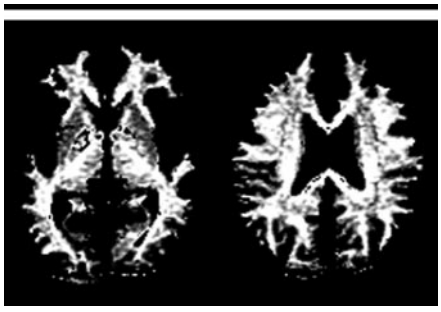

**Figure 1.** Successfully segmented WM FA map obtained by masking the native FA map with its own in-register high-probability WM binary mask.

ward either group. We first coregistered the non–diffusion-weighted image of each subject to a corresponding T1-weighted image by using mutual information coregistration. The T1-weighted image was then spatially affine normalized (by using 12 parameters: three translations, three rotations, three zooms, and three shears) to the CCHMC2_fp T1-weighted pediatric MR imaging template. The resultant affine transformation parameters were applied to the in-register non–diffusion-weighted MR images. All eight normalized non–diffusion-weighted images were averaged and smoothed by using an 8-mm isotopic Gaussian kernel to form a new non–diffusion-weighted pediatric image template. Each normalized non–diffusion-weighted image was segmented to yield three tissue probability maps: gray matter, WM, and cerebrospinal fluid (CSF) maps. All probability maps of each tissue class were averaged and smoothed by using an 8-mm isotopic Gaussian kernel. This process yielded a set of a priori probability maps for our non–diffusion-weighted MR image template.

### Quantitative Measure: Mean WM FA

Probability maps of gray matter, WM, and CSF for each subject were obtained (by L.H.T.L.) by segmenting the native non–diffusion-weighted MR images. Because the FA value was meaningful in only the WM tissue (6), we focused our study on the FA in WM tissue only. A WM binary mask image of each subject was required to mask out the WM FA map. A high-probability WM binary mask image was obtained by using three criteria in the image manipulation subroutine (ImCalc) in SPM99: *(a)* The probability value of WM was larger than the probability value of gray matter for a given tissue voxel ($i2 > i1$), *(b)* the probability value of WM was larger than the probability value of CSF of the same tissue voxel ($i2 > i3$), and *(c)* the probability value of WM was larger than the probability value of any tissue other than gray matter, WM, or CSF $\{i2 > [1 - (i1 + i2 + i3)]\}$, where $i1$, $i2$, and $i3$ represented values derived from the probability maps of gray matter, WM, and CSF, respectively. These criteria were used to examine each voxel and yielded a value of 1 or 0. A unity voxel denoted a WM voxel only if the sampling voxel fulfilled all three of these criteria. Any voxel that did not meet all of these requirements would be assigned a value of 0.

Because the FA map was derived from the non–diffusion-weighted MR images, the non–diffusion-weighted image and the FA map had identical voxel sizes, origins, and direction cosines and were in register. The WM binary mask image data could then be multiplied element-by-element by the in-register FA map data to produce a WM FA map (Fig 1). A histogram was derived from the WM FA map and normalized by using the total number of voxels that contributed to the histogram to compensate for differences in brain size. A quantitative index, the mean WM FA, was computed for each subject (by L.H.T.L.). As a result, four mean WM FA values for the control subjects in each of the four respective age groups (groups A–D) were calculated and used as control reference values for each age group.

### Statistical Analyses

The percentage change in WM FA (ΔFA) in each patient was calculated as follows: $\Delta FA = [(FA_p - FA_c)/(FA_c)] \cdot 100$, where $FA_p$ is the WM FA in the given patient and $FA_c$ is the mean WM FA for the age-matched control group. We evaluated the demographic data, treatment protocol, age at the time of CSI, time of MR imaging since CSI, and CSI dose, each in relation to the ΔFA in each patient (Table). Spearman rank correlation for nonparametric data was used to analyze the relationships between ΔFA and the factors age at CSI, time of MR imaging since CSI, and CSI dose. This analysis was followed by multiple linear regression analysis to study the simultaneous influence of these factors on ΔFA. All statistical analyses were performed by using a statistical software package (SPSS for Windows, version 11.0; SPSS, Chicago, Ill). $P < .05$ was considered to indicate statistical significance.

## RESULTS

### MR Image Data Processing

At visual inspection, we found no artifacts due to subject motion or instrument malfunction. We also found minimal eddy current–related distortions. The non–diffusion-weighted MR image segmentation results confirmed that the three tissue classes (WM, gray matter, and CSF) had been successfully segmented by using the SPM segmentation function in each patient in the final study cohort. An example of a final WM FA map with successful segmenting is shown in Figure 1.

### Mean WM FA in Control Subjects

The mean age of the control subjects was 6.8 years ± 1.1 (standard deviation) in group A, 9.3 years ± 1.0 in group B, 12.7 years ± 0.7 in group C, and 16.3 years ± 2.5 in group D. The mean WM FA value was 0.294 ± 0.016 in group A, 0.307 ± 0.013 in group B, 0.315 ± 0.012 in group C, and 0.335 ± 0.016 in group D.

### Mean WM FA in Patients

There were 14 male and six female patients, and their ages ranged from 5.2 to 18.6 years (mean age, 11.0 years ± 4.6). The ΔFA in the 20 patients, as compared with the mean WM FA value for the control subjects, ranged from −22.53% to 1.85% (mean, −4.8% ± 6.9). Fourteen (70%) of the 20 patients had reduced WM FA (mean reduction, 7.3% ± 6.9). For these 14 patients, the mean age at CSI was 7.5 years ± 3.8; the mean CSI dose, 35.4 Gy ± 3.0; and mean time of MR imaging since CSI, 2.8 years ± 2. For the remaining six patients with no reduction in WM FA, the mean age at CSI was 11.3 years ± 4.2; the mean CSI dose, 27.0 Gy ± 3.9; and the mean time of MR imaging since CSI, 1.4 years ± 1.3. Three of the 14 patients with reduced WM FA underwent MR imaging less than 1 year after CSI. The patients' demographic data, CSI doses, chemotherapy protocols, and ΔFA values are given in the Table.

At Spearman rank correlation analysis, there were significant associations between ΔFA and both age at CSI ($r = 0.631$, $P = .003$ [Fig 2]) and CSI dose ($r = -0.586$, $P = .007$ [Fig 3]) but not between ΔFA and time of MR imaging since CSI ($P = .726$). We noted outliers regarding two patients (Fig 2) (patients 2 and 3, aged 2.9 and 3.4 years, respectively, at CSI). At Spearman rank correlation performed after the removal of these pa-

**Demographic Data, Treatment Protocols, and WM Anisotropy Measurements for 20 Medulloblastoma Survivors**

| Patient No. | Age at MR Imaging (y) | CSI Dose (Gy) | Chemotherapy Protocol* | Age at CSI (y) | Time Since CSI (y)† | ΔFA‡ |
|---|---|---|---|---|---|---|
| 1 | 5.2 | 36.0 | CCV | 4.3 | 0.9 | −8.82 (−0.026/0.294) |
| 2 | 5.4 | 36.0 | POG | 2.9 | 2.5 | −22.53 (−0.066/0.294) |
| 3 | 5.5 | 36.0 | CCV | 3.4 | 2.1 | −22.35 (−0.066/0.294) |
| 4 | 6.4 | 23.4 | CCV | 5.8 | 0.6 | 1.53 (0.005/0.294) |
| 5 | 7.1 | 36.0 | POG | 5.7 | 1.4 | −10.10 (−0.030/0.294) |
| 6 | 7.2 | 30.6 | CCV | 4.9 | 2.3 | −5.55 (−0.016/0.294) |
| 7 | 8.1 | 36.0 | POG | 2.9 | 5.2 | −3.83 (−0.012/0.307) |
| 8 | 8.2 | 36.0 | CCV | 8.0 | 0.2 | −7.43 (−0.023/0.307) |
| 9 | 8.7 | 36.0 | CCV | 6.6 | 2.1 | −1.55 (−0.005/0.307) |
| 10 | 9.6 | 23.4 | CCV | 9.2 | 0.4 | 0.35 (0.001/0.307) |
| 11 | 11.0 | 23.4 | CCV | 10.7 | 0.3 | 0.12 (0.0004/0.315) |
| 12 | 12.0 | 40.0 | CCV | 10.6 | 1.4 | −1.70 (−0.005/0.315) |
| 13 | 12.8 | 30.6 | CCV | 12.1 | 0.7 | −4.89 (−0.015/0.315) |
| 14 | 12.9 | 30.6 | CCV | 9.9 | 3.0 | 0.18 (0.001/0.315) |
| 15 | 13.3 | 36.0 | POG | 7.5 | 5.8 | −3.67 (−0.012/0.315) |
| 16 | 13.7 | 40.0 | CCV | 8.0 | 5.7 | −3.35 (−0.011/0.315) |
| 17 | 17.7 | 30.6 | CCV | 14.8 | 2.9 | 1.85 (0.006/0.335) |
| 18 | 18.3 | 30.6 | CCV | 14.3 | 4.0 | −1.27 (−0.004/0.335) |
| 19 | 18.4 | 30.6 | CCV | 17.4 | 1.0 | 1.15 (0.004/0.335) |
| 20 | 18.6 | 36.0 | POG | 13.4 | 5.2 | −5.06 (−0.017/0.335) |

* CCV = lomustine, cisplatin, and vincristine treatment protocol; POG = authors' Pediatric Oncology Group protocol (ie, vincristine, cyclophosphamide, cisplatin, and etoposide).

† Time of MR imaging examination since CSI.

‡ Data are percentages. The numbers used to calculate the percentages are in parentheses. $\Delta FA = [(FA_p - FA_c)/(FA_c)] \cdot 100$, where $FA_p$ is the WM FA in a given patient and $FA_c$ is the mean WM FA for the age-matched control group. Because of the reduced number of decimal points in the ratio, the ratio may not be equivalent to the exact percentage.

tients' data, the correlations remained significant ($r = 0.515$ for correlation between ΔFA and age at CSI, $P = .029$; $r = -0.578$ for correlation between ΔFA and CSI dose, $P = .012$). Multiple linear regression analysis revealed only patient age at CSI to be an independent variable that significantly affected ΔFA (adjusted $r^2 = 0.391$, $P = .012$).

## DISCUSSION

Both age at CSI and CSI dose are well-recognized risk factors for radiation-induced WM damage in posttreatment brain tumor survivors. In our study cohort of medulloblastoma survivors, we found age at CSI to be an independent variable that affected WM anisotropy loss. CSI dose was found to be associated with changes in WM anisotropy at univariate analysis, but the effect of this variable was not significant when it was adjusted for age at CSI at multiple linear regression analysis. Although we expected higher CSI doses to cause more severe WM damage, the lack of a significant association may have been due to the small sample size in this study, which reduced the statistical power. Moreover, all but three of the patients who were treated for medulloblastoma received a radiation dose of 30 Gy or higher, and the variation in CSI dose among these patients was small.

The dose effect should be better assessed by comparing patients similar to those in our cohort with a group of patients who receive lower radiation doses, such as patients with leukemia, who receive less than 20 Gy of radiation at CSI. Nevertheless, our current results show that age at CSI is a more powerful variable than CSI dose in terms of the effect on WM anisotropy loss ($r = 0.631$ for age at CSI vs $r = -0.586$ for CSI dose). These associations with neurotoxicity risk factors support the fact that changes in WM anisotropy are related to treatment-induced neurotoxicity.

In our pilot study (5), we quantified FA by placing regions of interest in the WM in a small cohort of patients with medulloblastoma. Subsequently, we performed group comparisons of the whole-brain FA between patients and control subjects by using voxel-based analysis with SPM (6). We also studied differences between whole-brain and WM-only FA histograms and differences in histogram-derived indexes between the patient and control subject groups, but we did not quantify the WM ΔFA in individual patients for intersubject comparisons. Hence, we were not able to correlate FA changes with neurotoxicity risk factors in our previous study.

The quantitation of WM FA by using SPM segmentation, as compared with that performed by using region-of-interest placement, has the advantage of being reproducible and unbiased. Therefore, this method may be used in intersubject comparisons, as in the present study, and also for longitudinal follow-up. However, compared with the use of region-of-interest analysis, the use of SPM segmentation can result in an underestimation of the anisotropy loss because regions of interest are placed at central locations in the WM, which are more vulnerable to the damaging effects of radiation than peripheral WM regions (5,6). With WM segmentation, all WM regions, including the peripheral WM, are inadvertently included in the analysis, and, hence, there are volume-averaging effects from the normal WM. It is therefore likely that some patients with less severe anisotropy changes will not be identified with this method.

Seventy percent of our study patients—compared with all of the patients in our previous study, in which we used region-of-interest analysis—were found to have reduced anisotropy (5). In addition, the magnitude of FA reduction was less severe in this study (mean reduction, 7.3%) compared with that in our previous region-of-interest study (mean reduction, 18.4%) (5).

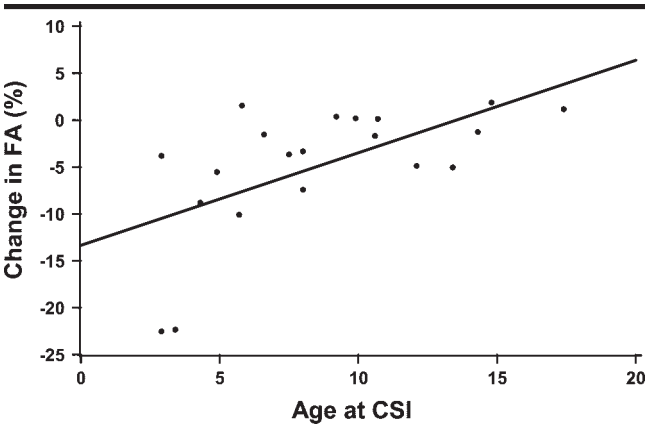


**Figure 2.** Scatterplot shows significant correlation between ΔFA and age at CSI in 20 medulloblastoma survivors (Spearman rank correlation, $r = 0.631$, $P = .003$).

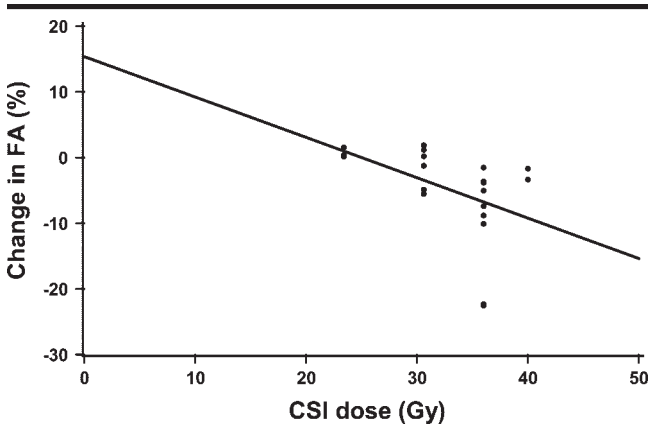


**Figure 3.** Scatterplot shows significant correlation between ΔFA and CSI dose in 20 medulloblastoma survivors (Spearman rank correlation, $r = -0.586$, $P = .007$).

Another limitation of the SPM WM segmentation method is failed segmentation. This may occur in subjects with large ventricles, as was the case with one patient in our current study, who was excluded from the final study cohort; in subjects with large subarachnoid spaces due to cerebral atrophy; and in subjects with severely distorted brain structures. Tissue classifications performed by using SPM segmentation would not be successful in these situations because the a priori probability images would be poor representatives of the image being segmented. For example, when ventricles are large, some ventricular voxels may be located where there is a 100% prior probability of the tissue being WM, and these CSF voxels would be misclassified as WM according to the SPM segmentation algorithm. On the WM FA map in Figure 1, several voxels are seen in the basal ganglia and thalami (ie, gray matter). This kind of tissue misclassification is due to the very similar probability values of the gray matter and the WM, which were derived by using SPM segmentation, and the thresholding technique used in making the binary mask. However, because our aim was to quantify the mean WM FA value, not the WM volume, we expected this overestimation of "WM" volume to cause only a slight underestimation of the mean WM FA.

Late radiation effects in the WM have been evaluated by using conventional T2-weighted MR imaging in animal model studies, and the findings of increased T2 relaxation times were attributed to vasogenic edema and demyelination (7–9,20). To our knowledge, similar studies to evaluate the diffusion characteristics of diffuse WM injury with diffusion-weighted or diffusion-tensor MR imaging have not been performed. Histologic studies of irradiated central nervous system specimens have revealed demyelination, proliferative and degenerative glial reactions, endothelial cell loss, and capillary occlusion (7–11,20). It is conceivable that the reduction in WM anisotropy reflects loss of integrity and disruption in microstructure of the axons related to these histologic changes.

Cognitive studies have revealed a progressive intellectual decline in medulloblastoma survivors at a rate of 2.05–4.30 intelligence quotient points per year (4,14–16). We found no significant association between time of MR imaging since CSI and ΔFA, which suggests that there is no progressive WM damage over time. However, larger patient numbers and longitudinal studies are needed to confirm this theory. Results of a relatively recent study of cognitive function in medulloblastoma survivors (16) indicated that the deterioration in intellectual function may be explained by the inability of an affected child to progress mentally at the same rate as his or her peers and the increasing demands placed on the child as he or she ages, rather than by a loss of previously acquired information and skills.

Although we did not evaluate the relationship between cognitive function and WM anisotropy in our patient cohort, investigators have observed correlations between cognitive function, especially cognitive decline, and FA in other types of cohorts (21). Moreover, a study involving medulloblastoma survivors revealed that some cognitive functions—namely, attention ability—are related to WM volume loss; this finding indicates that the WM may be the underlying mechanism of cognitive decline (22,23). Hence, it is possible that other parameters of WM disease, such as anisotropy loss, also may correlate with cognitive function.

In this cross-sectional study, a loss of anisotropy was observed in three of the six patients who were examined less than 1 year after treatment. This finding suggests that anisotropy loss may be detected as early as within 1 year after irradiation. Anisotropy loss may therefore be an early indicator of WM damage, and, if the anisotropy value is measured during or before the completion of treatment, it may be used as a parameter to effect change in the treatment strategy. This measurement is in contrast to cognitive examinations, which tend to be performed at least 1 or 2 years after treatment and only after neurotoxicity has developed. Therefore, further diffusion-tensor MR imaging examinations should be performed to evaluate FA changes before treatment and at early time points during the course of treatment so that the timescale for WM changes can be characterized. Ideally, an FA threshold for brain injury should be determined at early time points.

Our study was limited by the use of groups of control subjects of a given (albeit small) age range—rather than an exact age—whose mean data were matched with those of individual patients. Study results have shown that the greatest change in brain water diffusion occurs during the first 4 years of life and that the increase in WM anisotropy is nonlinear, with the highest increase occurring during the first few years and the measurement reaching an asymptotic level at about 6 years in the internal capsule and

the corpus callosum and at about 8 years in the peripheral WM of the centrum semiovale (24–27). Hence, it is possible that we overestimated the degree of reduction in WM FA in the patients younger than 6 years in our study because we compared them with a control group of subjects with a mean age of 6.8 years. Finally, correlation of the FA changes with the neuropsychologic data of these patients is essential for determining both the clinical relevance of reduced WM FA and the usefulness of diffusion-tensor MR imaging in the assessment of treatment-induced neurotoxicity.

In conclusion, we found age at CSI to be an independent variable that affected WM anisotropy loss in posttreatment medulloblastoma survivors and observed a trend toward increasing anisotropy loss with larger CSI dose. Although it is not clear how these observations of reduced WM anisotropy reflect the cognitive outcomes of patients who have been treated for medulloblastoma, determining the mean WM FA value is potentially a useful outcome measure for evaluating treatment-induced neurotoxicity and may also be used for assessing the timing and application of neurotoxic treatments.

**Acknowledgments:** The authors thank the radiographers in the radiology department of Queen Mary Hospital for their invaluable help with this project.

**References**

1. Packer RJ, Sposto R, Atkins TE, et al. Quality of life in children with primitive neuroectodermal tumors (medulloblastoma) of the posterior fossa. Pediatr Neurosci 1987; 13:169–175.
2. Johnson DL, McCabe MA, Nicholson HS, et al. Quality of long-term survival in young children with medulloblastoma. J Neurosurg 1994; 80:1004–1010.
3. Silverman CL, Palkes H, Talent B, Kovnar E, Clouse JW, Thomas PRM. Late effects of radiotherapy on patients with cerebellar medulloblastoma. Cancer 1984; 54:825–829.
4. Walter AW, Mulhern RK, Gajjar A, et al. Survival and neurodevelopmental outcome of young children with medulloblastoma at St Jude Children's Research Hospital. J Clin Oncol 1999; 17:3720–3728.
5. Khong PL, Kwong DL, Chan GC, Sham JS, Chan FL, Ooi GC. Diffusion-tensor imaging (DTI) for the detection and quantification of treatment-induced white matter injury in children with medulloblastoma: a pilot study. AJNR Am J Neuroradiol 2003; 24:734–740.
6. Leung LH, Ooi GC, Kwong DL, Chan GC, Cao G, Khong PL. White-matter diffusion anisotropy after chemo-irradiation: a statistical parametric mapping study and histogram analysis. Neuroimage 2004; 21:261–268.
7. Benczik J, Tenhunen M, Snellman M, et al. Late radiation effects in the dog brain: correlation of MRI and histological changes. Radiother Oncol 2002; 63:107–120.
8. Miot E, Hoffschir D, Alapetite C, et al. Experimental MR study of cerebral radiation injury: quantitative T2 changes over time and histopathologic correlation. AJNR Am J Neuroradiol 1995; 16:79–85.
9. Kennedy AS, Archambeau JO, Archambeau MH, et al. Magnetic resonance imaging as a monitor of changes in the irradiated rat brain. Invest Radiol 1995; 30:214–220.
10. Ruifrok AC, Stephens LC, van der Kogel AJ. Radiation response of the rat cervical spinal cord after irradiation at different ages: tolerance, latency and pathology. Int J Radiat Oncol Biol Phys 1994; 29:73–79.
11. Calvo W, Hopewell JW, Reinhold HS, Yeung TK. Time- and dose-related changes in the white matter of the rat brain after single doses of x rays. Br J Radiol 1988; 61:1043–1052.
12. Silber JH, Radcliffe J, Peckham V, et al. Whole-brain irradiation and decline in intelligence: the influence of dose and age on IQ score. J Clin Oncol 1992; 10:1390–1396.
13. Mulhern RK, Kepner JL, Thomas PR, Armstrong FD, Friedman HS, Kun LE. Neuropsychologic functioning of survivors of childhood medulloblastoma randomized to receive conventional or reduced-dose craniospinal irradiation: a pediatric oncology group study. J Clin Oncol 1998; 16:1723–1728.
14. Palmer SL, Gajjar A, Reddick WE, et al. Predicting intellectual outcome among children treated with 35–40 Gy craniospinal irradiation for medulloblastoma. Neuropsychology 2003; 17:548–555.
15. Ris MD, Packer R, Goldwein J, Jones-Wallace D, Boyett JM. Intellectual outcome after reduced-dose radiation therapy plus adjuvant chemotherapy for medulloblastoma: a children's cancer group study. J Clin Oncol 2001; 19:3470–3476.
16. Palmer SL, Goloubeva O, Reddick WE, et al. Patterns of intellectual development among survivors of pediatric medulloblastoma: a longitudinal analysis. J Clin Oncol 2001; 19:2302–2308.
17. Basser PJ. Inferring microstructural features and the physiological state of tissues from diffusion-weighted images. NMR Biomed 1995; 8:333–344.
18. Basser PJ, Mattiello J, LeBihan D. MR diffusion tensor spectroscopy and imaging. Biophys J 1994; 66:259–267.
19. Wilke M, Schmithorst VJ, Holland SK. Assessment of spatial normalization of whole-brain magnetic resonance images in children. Hum Brain Mapp 2002; 17:48–60.
20. Grossman RI, Hecht-Leavitt CM, Evans SM, et al. Experimental radiation injury: combined MR imaging and spectroscopy. Radiology 1988; 169:305–309.
21. Shenkin SD, Bastin ME, MacGillivray TJ, Deary IJ, Starr JM, Wardlaw JM. Childhood and current cognitive function in healthy 80-year-olds: a DT-MRI study. Neuroreport 2003; 14:345–349.
22. Mulhern RK, Palmer SL, Reddick WE, et al. Risks of young age for selected neurocognitive deficits in medulloblastoma are associated with white matter loss. J Clin Oncol 2001; 19:472–479.
23. Mulhern RK, Reddick WE, Palmer SL, et al. Neurocognitive deficits in medulloblastoma survivors and white matter loss. Ann Neurol 1999; 46:834–841.
24. Nomura Y, Sakuma H, Tagami T, Okuda Y, Nakagawa T. Diffusional anisotropy of the human brain assessed with diffusion-weighted MR: relation with normal brain development and aging. AJNR Am J Neuroradiol 1994; 15:231–238.
25. Morriss MC, Zimmerman RA, Bilaniuk LT, Hunter JV, Haselgrove JC. Changes in brain water diffusion during childhood. Neuroradiology 1999; 41:929–934.
26. Mukherjee P, Miller JH, Shimony JS, et al. Normal brain maturation during childhood: developmental trends characterized with diffusion-tensor MR imaging. Radiology 2001; 221:349–358.
27. Philip JV, Mukherjee P, Neil JJ, McKinstry RC. White matter maturation in older children demonstrated with diffusion tensor MRI (abstr). In: Proceedings of the Ninth Meeting of the International Society for Magnetic Resonance in Medicine. Berkeley, Calif: International Society for Magnetic Resonance in Medicine, 2001; 409.